Applied Materials Today 26 (2022) 101265

Contents lists available at ScienceDirect

Applied Materials Today

journal homepage: www.elsevier.com/locate/apmt

Reconfigurable and regenerable liquid metal surface oxide for continuous and quantifiable adsorption of biological dye

Xinpeng Wang[a], Hongzhang Wang[b], Kang Sun[a], Wanjun Li[c], Xuelin Wang[a], Xuanqi Chen[a], Liang Hu[a,*], Yubo Fan[a,*]

[a] Beijing Advanced Innovation Center for Biomedical Engineering, School of Biological Science and Medical Engineering, Key Laboratory for Biomechanics and Mechanobiology, Beihang University, Beijing 100191, China
[b] Department of Biomedical Engineering, School of Medicine, Tsinghua University, Beijing 100084, China
[c] Chongqing Key Laboratory of Photo-Electric Functional Materials, College of Physics and Electronic Engineering, Chongqing Normal University, Chongqing 401331, China

ARTICLE INFO

Article history:
Received 26 July 2021
Revised 15 October 2021
Accepted 7 November 2021

Keywords:
Reconfigurable metal oxide
Liquid metal
Gallium
Ponceau S
Dye adsorption

ABSTRACT

Among water purification techniques, adsorption is one of the most effective and economical methods. However, the adsorbents are usually static materials, which are faced with issues such as regeneration and recovery difficulties. Here we report a reconfigurable and sustainable liquid metal oxide as adsorbent for effectively removal of a common azo dye, Ponceau S (PS), in water. Gallium-based alloy (GaInSn) with excellent reconfigurability and fluidity at room temperature is revealed to continuously produce surface gallium oxide for PS adsorption by simply mild shaking or stirring. The adsorption process is fast and energy saving in water. Besides, the oxide is easily removed from wastewater by taking out the whole liquid metal. Moreover, combined with electrical conductivity of liquid gallium, the impedance alteration after PS adsorption can be characterized by impedance sensing technique, which offers an electrical quantification method for PS absorption. This study put forward a unique way for the design and fabrication of adsorbents with continuous and multifunctional performance. Moreover, it will inspire more possible applications of reconfigurable materials in the fields of dye adsorption, environmental engineering and even detection methods for molecular monitoring.

1. Introduction

Reconfigurable materials that are capable of changing their structures, appearance and other properties on-demand are becoming an emerging theme in material science. Owning to their inherent or predesigned deformability in responding to various tasks or conditions [1], reconfigurable materials have presented broad prospects in applications such as drug delivery [2], biomedical engineering [3,4], intelligence antenna [5], soft robotics [6] and so on [7,8]. Even so, increasing effort are still made in developing new reconfigurable materials, structures and systems, which may exert great values in more potential applications.

Water pollution is already becoming a global issue for the 21st century, in which dye effluent is one of main pollutants. Among all dye types, azo dyes are the highest produced dye type at 70% production rate and it is the most frequently utilized dye worldwide [9]. Ponceau S (3-hydroxy-4-(2-sulfo-4-[4-sulfophenylazo]phenylazo)-2,7-naphthalene disulfonic acid sodium salt, PS), one of azo dyes, is widely used in textile, leather, paper industries and biological staining [10,11]. Meanwhile, PS dye is also an important pollutants in water pollution worldwide and is declared as II-cancerogen by World Health Organization International Agency for Research on Cancer [12,13]. Among various water purification techniques developed in dye removal, adsorption is one of the most effective, economical and convenient method [14–17]. Various adsorbents have been developed for the removal of PS, including magnesium oxide (MgO) nanoparticles [18], graphene oxide (GO) [19], aluminum phosphate ($AlPO_4$) [20], clays [21] and some polymers [22–24]. Despite their excellent performance in dye adsorption, the recovery or regeneration remains an issue, as shown in Table 1. For instance, these two-dimensional (2D) materials or nanomaterials usually have low recovery rate due to the large surface area interaction, and often cause secondary pollution. Moreover, the raw synthetic adsorbents need extra preparation process or surface modification, which is complex, energy-consuming, or environmentally unfriendly, requiring more chemical engineering cost.

* Corresponding authors.
E-mail addresses: cnhuliang@buaa.edu.cn (L. Hu), yubofan@buaa.edu.cn (Y. Fan).

https://doi.org/10.1016/j.apmt.2021.101265
2352-9407/

Table 1
Comparison of adsorption capacity of different adsorbents toward PS dye.

Adsorbents	q_{max} (mg/g)	Advantages	Disadvantages	Ref.
MgO nanoparticles	93.02	Improved adsorption capacity	Complex recovery process	[18]
Nanosized niobium pentoxide with activated carbon	41.05	Improved adsorption capacity	Hard recovery, need to further improve adsorption capacity	[49]
PDDA-modified GO	188.679	Improved adsorption capacity	High cost of GO	[19]
SDBS-modified $AlPO_4$	60.8	Improved adsorption capacity	Hard recovery, complex preparation process	[20]
Organic clay	0.07 mg/L	Ease production and relatively low cost	Poor recycling	[21]
Polyethylenimine modified Fe_3O_4 nanoparticles	140.26	Improved adsorption capacity, magnetic removal	Hard recovery, complex preparation process	[50]
PDA/PEI@PVA/PEI nanofibrous membranes	1180	Strong adsorption capacity	Complex preparation process	[24]
Ga/GaIn/GaInSn	At least 50 mL PS/100 μL LM (about 83.3 mg/g)	Reconfigurable ability, Simple preparation process, Easy to recycle, Conductivity and adsorption can be used for real-time monitoring	High density	Present work

Herein, we present a reconfigurable and sustainable liquid metal oxide as a brand-new adsorbent for continuous adsorption of Ponceau S. Here, gallium-based alloy, GaInSn, with excellent fluidity and transformability at room temperature [25–27] can continuously produce oxide layer for PS adsorption by simply mild shaking or stirring. In this regard, the gallium oxide skin over the flowing liquid metal (LM) is easily reconfigurable and continuously producible. The adsorption process is fast and energy saving in water. The mechanism of adsorption is analyzed preliminarily, showing during the adsorption the oxide layer acts as an adsorbent via electrostatic attraction, π-π interaction, intercalative binding and H-bonding at pH < 10, while the Ga ions should play the role of promotion. Moreover, gallium/EGaIn/GaInSn were contrasted, proving that gallium-based alloys own the capacity for this dye adsorption. And the solidified gallium was also proved the feasibility, which was easily to be taken out and recycled to be used in wide ambient environment. As a proof-of-concept, considering the change of surface tension, the impedance during adsorption process was detected, which could be used to detect the concentration. Obviously, this work will open opportunities of gallium-based liquid metals in adsorption, surface modification, environmental engineering, molecular monitoring, and provide a new way of thinking for biomedical detection.

2. Materials and methods

2.1. Materials

The eutectic liquid-metal alloys (GaInSn, Ga 68.5%, In 21.5%, Sn 10% by mass, and EGaIn, Ga 75%, In 25% by mass) were prepared from gallium, indium, and tin with purity of 99.99%. These raw materials with mass ratios of 68.5:21.5:10 and 75:25 were added into a beaker and were heated to 100 °C to form the mixture uniformly. The alloy was used in the subsequent experiments. Ponceau S stain reagent (PS) was purchased from EpiZyme and used as received without further purification. Acetic acid (HAc), Gallium (III) nitrate hydrate (Aladdin) were used to prepare the solvent, Ga ion solution and prove the adsorbability of Ga ion. NaCl, HCl and NaOH were used to adjust ion strength and pH, separately. Deionized water (Milli-Q System, Millipore, USA) was used in all experiments.

2.2. Characterization

The Ultraviolet-visible (UV-Vis) spectra were obtained by an absorbance spectrometer (Thermo Scientific ™ Varioskan ™ LUX). The morphology of LM and the prepared and dried powders were characterized using a field-emission scanning electron microscope (FESEM, JSM-7100F, JEOL, Peabody, MA, USA). And elemental analysis was examined by energy dispersive spectrometer (EDS). An ESCALAB 250 XPS (Thermo Fisher Scientific Company, USA) was used to test the change of chemical compositions and oxidation states on LM before and after adsorption. FT-IR spectra were recorded on a Fourier transform infrared (FT-IR, CARY670, Agilent, Santa Clara, CA, USA) spectrometer to analyze the chemical bonding of the product in the wavenumber range of 4000–400 cm^{-1}. X-ray diffraction (XRD, -7000, Tokyo, Japan) with Cu Kα radiation ($\lambda = 0.154$ nm) was used to examine the structure and crystallinity of the synthetic product using powder. The impedance between GaInSn and PS was measured on an electrochemical workstation (CHI660E, USA) within a frequency range from 0.1 to 1000 Hz.

2.3. Adsorption capability test

In order to research the adsorption capability for dyes from water pollution, the influence of the ratio of GaInSn and PS, pH (2, 3, 4, 5, 7, 9, 11, 12), shaking frequency (10, 20, 30, 40, 50, 60 round/min, with 20° shaking angle), temperature (20, 25, 35, 45, 55, 65 °C), ionic strength (0 M, 0.1 M, 0.25 M, 0.5 M, 1.0 M, 2.0 M) or cycle number in the adsorption process was further investigated. Six kinds of LM/PS with different ratios (0.2:1, 0.4:1, 0.6:1, 0.8:1, 1:1, 2:1, v/v) were prepared, with the concentration of PS dye solutions (1000 μL, 1 g/L, pH = 2.5).

The mixtures were shaken at a 20-degree angle until the solution changing from red to colorless and then centrifuged for 20 s at 5000 rpm. The supernatants were detected by the UV-Vis absorbance spectrometer. For PS solutions, the concentration was separately determined by the absorbance at 506 nm in the UV-Vis spectrum ($\varepsilon = 1.05 \times 10^4$ mol•L^{-1}•cm^{-1}). All the experiments were carried out at room temperature (25 ± 1 °C).

The removal efficiency of the dyes was calculated according to the Eq. (1):

$$\text{Removal efficiency}\ (\%) = \frac{(C_0 - C_e)}{C_0} \times 100 \quad (1)$$

where C_0 and C_e are the initial and equilibrium concentration of dye solutions, respectively.

To assess the sustainable stability of this adsorbent, at the equilibrium time we used the deionized water rinse the LM and then add the PS solution again to evaluate the repeatability. In these processes, GaInSn was used through all the experiments.

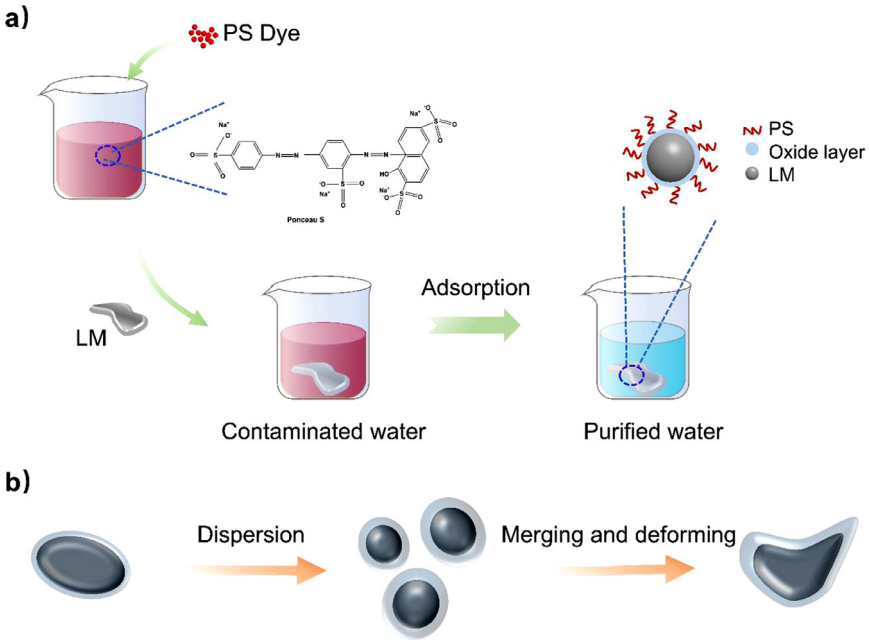

Fig. 1. Adsorption process on PS of LM (a), merging and deformation process of reconfigurable liquid metal (b).

In order to explore the universality of adsorption process of gallium and its alloys, EGaIn and solid Ga were separately put into PS solutions. And as a control group, to prove the adsorption ability and illustrate the influence of Ga ion, Gallium (III) nitrate hydrate (Aladdin) were added into the PS solution separately.

2.5. Impedance test

In order to investigate the electrochemical properties of the adsorption process, the self-made electrode solution catheter was made. In a 5 cm silicone tube (inner diameter 2 mm), 200 μL PS solution was thrusted into the tube (about 3.2 cm). And then, as the detected electrode, GaInSn was injected at both side (respectively about 0.9 cm). Electrochemical Impedance Spectroscopy (EIS) was setting (0.1 to 1000 Hz) at 5 mV to detect the impedance change at different time during the adsorption process.

3. Results and discussion

The whole adsorption process of liquid metal with significant reconfigurable ability could be schematically illustrated as Fig. 1. Firstly, as the instruction in western blotting, PS solution (1 g/L) was prepared with acetic acid (5%, v/v) and deionized water. Subsequently, liquid metal (GaInSn/EGaIn/Ga) was added into the solution. Then, without heating, the solution was adsorbed from red color to colorless (around 3 min, under LM:PS = 1:1 and shaking frequency 60 round/min at 25 °C). As described in the previous research, gallium, as the strongest Brønsted acid of the group 13 metals, will produce Ga ions into deionized water [28]. And then the following reactions (2)–(9) will occur in the exist of oxygen (ppm level) and water [28–31].

$$Ga(l) + O_2(g) \rightarrow Ga_2O_3(s) \quad (2)$$

$$Ga + H_2O \overset{ROS,\ \Delta}{\rightarrow} GaOOH \quad (3)$$

$$2Ga_2O_3 + H_2O \rightarrow 4GaOOH \quad (4)$$

$$GaOOH + H_2O \rightarrow Ga^{3+} + 3OH^- \quad (5)$$

$$[Ga(H_2O)_6]^{3+} + H_2O \rightarrow [Ga(H_2O)_5OH]^{2+} + H_3O^+ \quad (6)$$

$$[Ga(H_2O)_5OH]^{2+} + H_2O \rightarrow [Ga(H_2O)_4(OH)_2]^{+} + H_3O^+ \quad (7)$$

$$[Ga(H_2O)_4(OH)_2]^{+} + H_2O \rightarrow Ga(OH)_3 + H_3O^+ \quad (8)$$

$$Ga(OH)_3 \rightarrow GaOOH + H_2O \quad (9)$$

It is worth noting that the Ga reacts slowly with water to produce H_2 at room temperature. Based on the experimental phenomenon, after adding GaInSn, it is found that the PS solution will change from red to colorless when pH < 10, while change from red to bright yellow when adjusting pH ≥ 10. Considering the surface electrical behavior of gallium (electropositive) and PS (anionic dye), it is assumed that the adsorption process is determined by two situations. As illustrated in Scheme 1, on the one situation, due to the electrostatic attraction, PS molecules (negative ion) are attracted by the liquid metal with positive potential. And obviously, PS molecules could be adsorbed via H-bonding. Intermolecular π-π interaction also promotes the adsorption process. Moreover, due to the defect structure of oxide layer [32], the PS molecules can be adsorbed into the structure, which is called intercalative binding. Above all, from this situation, these interactions including electrostatic attraction, π-π interaction, intercalative binding and H-bonding are physical process. The PS solution, thus, changes from red color to colorless (Figs. 2a and **S1**). **Movie 1** illustrates this process. On the other situation, the PS molecules maybe interact with oxide layer to produce a new product (bright yellow color) when pH ≥ 10 [33,34], which should be a chemical reaction and will provide a new idea for chemical synthesis. In this study, we focus on the first respect, a physical adsorbed process (pH < 10).

Compared with GaInSn, EGaIn (Fig. S2a) and Ga (Fig. 2b and **Movie 2**) showed similar adsorption ability. It implies that the adsorption is related to gallium element, which suggests most gallium-based alloys own the capacity for this dye adsorption. It is well known that different gallium-based alloys own different properties [35–37], which could be applied in various conditions.

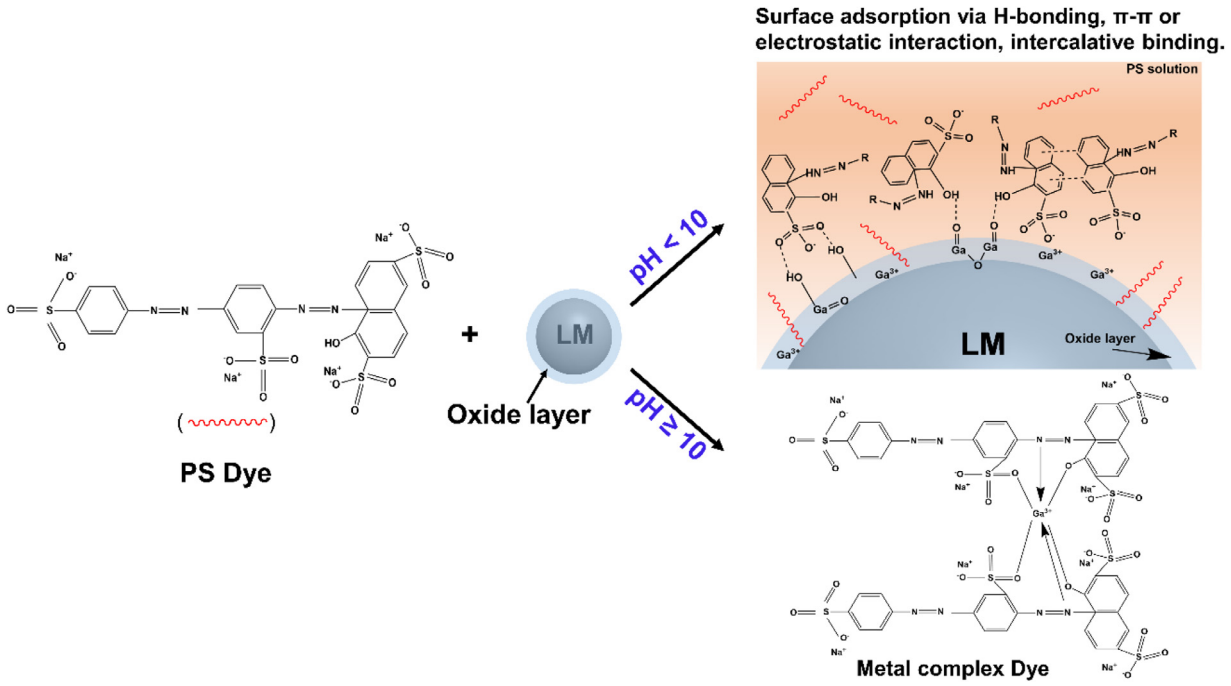

Scheme 1. Schematic presentation of adsorption process and reaction.

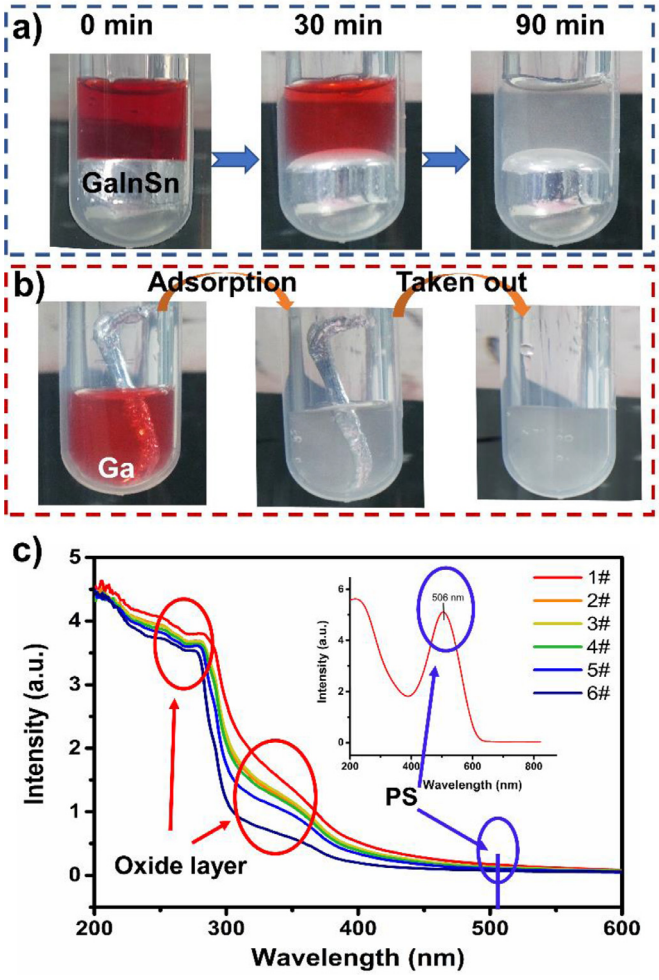

Fig. 2. Images of adsorption of GaInSn (a). Photos of adsorption and taken out of solid Ga (b). UV-Vis spectrum from 200–600 nm of different LM/PS ratio 1-6 # (0.2:1, 0.4:1, 0.6:1, 0.8:1, 1:1, 2:1, v/v, in sequence) (c), with the UV-Vis spectra of PS inside.

Table S1 lists the physical properties of several typical liquid metals. For example, it can be seen that, EGaIn and GaInSn with lower melting point (15.7 and 10.5 °C) and greater degree of supercooling than pure Ga, could be used in sub-zero lower conditions once melted, still keeping liquid state in wide range to adsorb the dye solution in an irregular container. Moreover, from the experimental results, it could be concluded that the adsorption process will be promoted under high temperature. Therefore, GaInSn with greater thermal conductivity is beneficial to the adsorption. Notably, once solidified, pure gallium is solid at room temperature, with melting point 29.8 °C. As shown in Fig. 2b and **Movie 2**, solid gallium still could adsorb the dye. After adsorption, the solid gallium could be removed and recycled conveniently. This phenomenon reveals that these reconfigurable metals, no matter solidified or melted, provide more applicated values no matter in normal environment but also extreme environment.

To interpret the underlying mechanism of this adsorption, we explore and characterize three parts: the components in the supernatant, the surface morphology of LM and the oxide layer. The components in the supernatant are detected by the UV-Vis. Fig. 2c shows the adsorption spectrum from 200 nm to 600 nm. Compared with the PS solution itself (inside Figs. 2c and **S2**b), it could be seen clearly that the PS has been adsorbed (without peak at 506 nm), with the peak intensity changed from 5 to near zero. According to the previous characterization [38], the peak at around 290 and 350 nm could be distinguished as the intrinsic absorption and sub-band absorption respectively of gallium oxide. The sub-band absorption should be related with the existence of abundant defect sites in gallium oxide. The peak intensity approximately decreases with the increasing of LM/PS ratio. It may be because PS molecules enhance the interaction of oxide layers to form big layers, not existing in the supernatant after centrifugation. Moreover, there is no other peaks appeared, which showing no new product in the supernatant. Thus, the change after the adsorption of PS should be on the surface of LM. To examine the surface morphology of LM after adsorption, field-emission scanning electron microscope (FESEM) is used. As shown in Fig. 3a, compared to the surface morphology in water (Fig. 3b), after adsorption of PS, the surface has more winkles and thicker. It is verified by the EDS re-

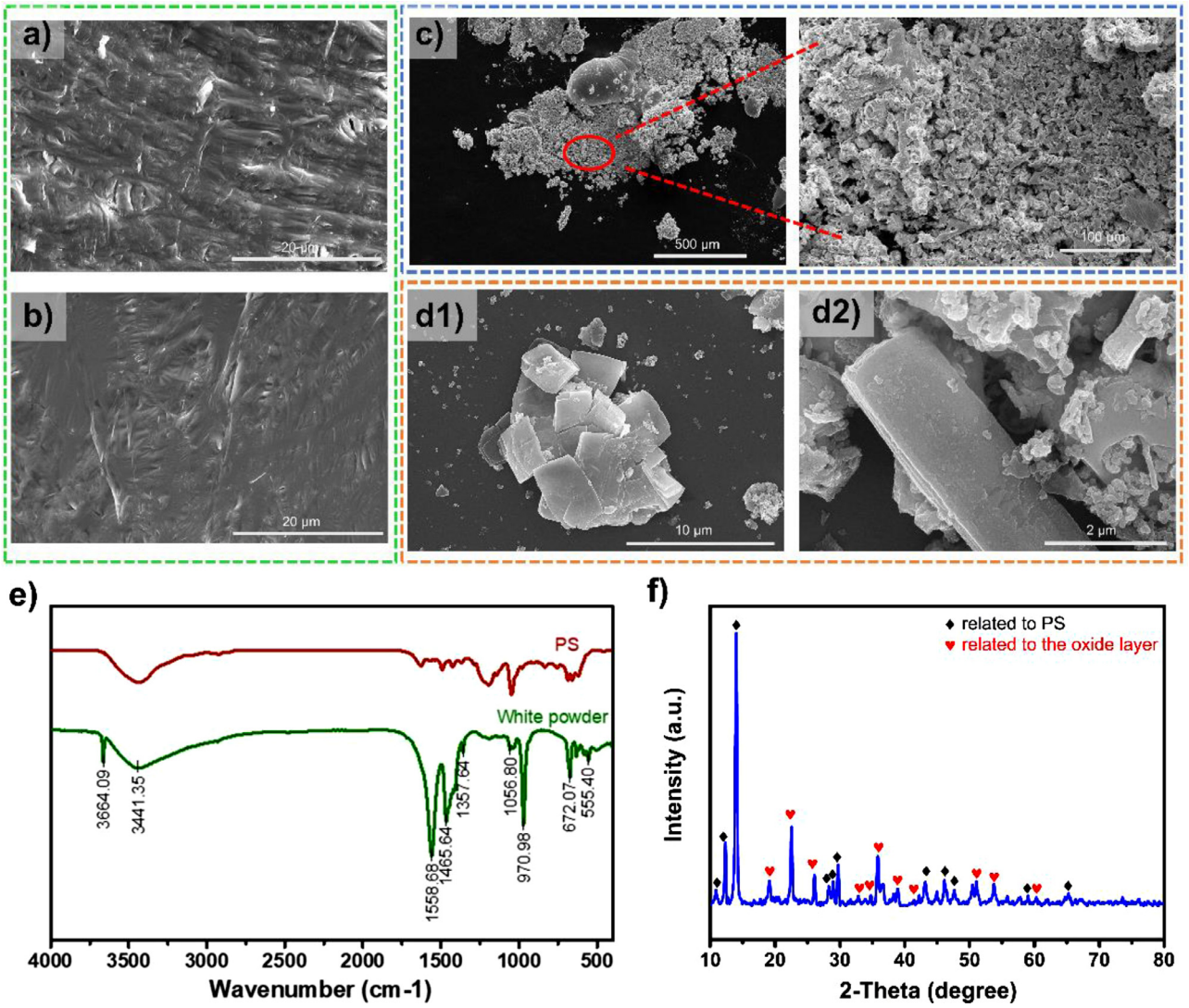

Fig. 3. SEM of oxide layer after adsorption of PS (a) and in water (b), white precipitate powder (c,d) at different magnification and different shape. FT-IR (e) and XRD (f) of white precipitate powder.

sult (Fig. S3 and Table S2), which reveals that the surface layer after adsorption of PS contains more element of oxygen (24.82%) than LM in water (11.60%) and in air (10.44%). To further study the interaction and oxidation states after adsorption, the binding states of elements on the surface of LM were measured by XPS. As shown in Fig. S4, XPS survey spectrum after adsorption reveals the surface structure primarily includes gallium, carbon, nitrogen, and oxygen elements. Peaks at binding energy of 20.1, 19.2 and 17.6 eV in XPS spectrum of Ga 3d can be assigned to Ga^{3+}, Ga^{+} and metallic gallium (Ga^{0}) respectively, which indicates the formation of a gallium oxide "skin" and probably some Ga (III) ions adsorbed onto the surface of LM. For O 1s spectrum, the peak at 530.8 eV is referred to O - Ga signals [39]. And the peaks at 530.1 and 531 eV are referred to hydrated -OH and non-hydrated -OH, respectively [40]. The N 1s spectrum shows binding energy at 395.7 eV corresponding to the signals of N-C. More importantly, the contribution from N 1s of binding energy at 397.0 eV was also observed, which was assigned to N - Ga moiety [39]. The C 1s region is fitted with four components at 291.2 eV ($\pi - \pi^*$), 288.6 eV (C=O), 285.7 eV (C–N, C–O), and 284.6 eV (C–C, C=C), which corresponds well with PS structures [41]. Moreover, compared the surface element states with LM in water and in air (Fig. S5), it shows slightly more oxygen element after adsorption, which is consistent with the result of EDS. Overall, these data verify that PS was adsorbed onto the surface of LM. Moreover, after dried, the surface layer showed more flatness and integration as revealed in Fig. S6, which probably because of the connecting effect of PS. These results above prove the existence of gallium oxide layer, which implies that the adsorption is related to the oxide layer.

Furthermore, taking the LM/PS ratio (1:1) as an example, we collect the white powder (the oxide layer) on the surface of LM after adsorption to observe the surface morphology (Fig. 3c,d), analyze the chemical bonding (Fig. 3e), and examine the structure and crystallinity (Fig. 3f), using SEM, Fourier transform infrared (FT-IR) and X-ray diffraction (XRD), respectively. From the morphological figures of plicated powder (Fig. 3c), it can be seen that the oxide layer at high magnification (Fig. 3d) is with different shapes, which is consistent with the morphology of gallium oxide in the precious reports [42]. More detailed characterization by SEM/EDS in Fig. S7a and Table S3 could be seen. The powder has abundant elements of O/C, which could be inferred that PS was on the oxide layer. To know more about the chemical bonding between PS and gallium oxide, PS and the white powder were characterized by FT-IR. As illustrated in Fig. 3e, the same amount pure PS sample was used as the blank control sample. As shown in the curves of PS and white powder, the broad bands at 3441 cm^{-1} reveals

abundant O-H stretching vibrations. Here, the O-H stretching vibrations was enhanced due to the hydrogen - bond interaction after adsorption. After conjugation of PS with LM, the peaks arising from -N=N- and benzene ring group are visible at around 1558 and 1465 cm^{-1} [33,43], which related to the π-π interaction between PS to some extent. And it can be seen that, the bands corresponding to the Ga-O stretching modes were observed at 825, 660 and 484 cm^{-1}. In addition to Ga-O mode, the bands at 2065–2092 cm^{-1}, together with bands at 1056 and 970 cm^{-1} are attributed to the Ga-OH bending modes. Since the peak position of Ga-OH deformation modes and Ga-O stretching modes were sensitive to pH and thermal treatment of the materials [43]. Therefore, the peak position is slightly offset. Totally, after conjugation of PS with LM, the peaks intensity of Ga-O and benzene ring are enhanced, which indicates that the successful combination of PS and oxide layer. And in the curve of white powder, there is a new peak at 3664 cm^{-1}, maybe because of water molecules bonded with the GaO(OH) hydroxyl units. From the result of FT-IR, it could be seen that there are no other new bond types formed after adsorption, which proved the adsorption is physical process (electrostatic attraction, π-π interaction, intercalative binding and H-bonding) consistent with the hypothesis. To know the difference with different LM/PS ratios, FT-IR and images of white supernatant powder with different LM:PS ratios (1-6 represent 0.2:1, 0.4:1, 0.6:1, 0.8:1, 1:1, 2:1, v/v, in sequence) were shown in Fig. S7b. It could be seen that the peak of O-H stretching vibrations will not be enhanced until LM/PS ratio is 0.6:1, which may be due to the hydrogen - bond interaction between PS and gallium oxide is saturated. And since the gallium-based liquid metals are stable under certain levels of oxidation, the oxide layer (~1–7 nm) will not continue to increase [44–46]. Therefore, the intensity of the peaks will not keep increasing all the time. Relevant confirmatory experiments will be further explored in subsequent studies. As described above, FT-IR spectroscopy clearly indicates the successful combining of the oxide layer and PS, which confirms that the adsorbent is the oxide layer. Based on the XRD characterization of gallium oxide hydroxide (GaOOH) [42,43], Fig. 3f reveals that the sample contains groups of both PS and oxide layer. It also suggests that the combination of PS and oxide layer, which further proves the oxide layer performs as an adsorptive function. Furthermore, considering the urgent need to prepare Ga_2O_3/GaOOH in semiconductor industry, this method provides a convenient way to forming functional composites.

To be better quantify the adsorption process, the ratio of GaInSn and PS, pH, shaking frequency, temperature, ionic strength and cycle number in the adsorption process were further investigated separately as described in experimental section. As illustrated in Fig. 4a,b, with the increasing of ratio (LM:PS) and shaking frequency, the adsorption time is shortened in a linear relation. Even under shaking, the adsorption equilibrium time could be greatly shortened from about 150 min (without shaking) to 200 s. As increasing of liquid metal and then promoting the reaction (2)–(9), the positive charge and the oxide layer forming increases. Under shaking, molecular motion is accelerated and the surface contact area is increased, so that oxygen content and molecular contact time increase. In a word, the increasing of LM or shaking frequency promote the formation of the oxide layer, which further proved the adsorption is related to the formation of oxide layer. As known that pH is a vital factor to form gallium oxide layer. as shown in Fig. 4c, at different pH, the adsorption has different phenomenon. From the appearance of the phenomenon, the red PS solution could be adsorbed into colorless in an acid and neutral environment, while into bright yellow color in an alkaline environment. In a neutral environment, the red PS solution could be adsorbed into colorless, and then the solution quickly turned into light red. Moreover, we found that the adsorbed performance of gallium-based metal and gallium salt with the same Ga concentration was different. As the control group, it was proved that Ga ion alone could not adsorb PS in three days or long time. This difference between liquid metal solution and pure Ga ion solution is consistent with the previous studies, which indicate that EGaIn exposure could promote producing reaction oxygen species (ROS) [47]. As we know, ROS include a number of reactive molecules and free radicals derived from molecular oxygen, which include hydrogen peroxide (H_2O_2), superoxide anions ($\bullet O_2^-$), hydroxyl radicals (•OH), singlet oxygen ($^1O_2$), and alpha-oxygen (α-O). These molecules show the potential to promote reaction (3). And as shown in Scheme 1, production of GaOOH will promotes the adsorption process. Thus, we propose that during the adsorption the oxide layer acts as an adsorbent, while the Ga ions plays the role of promotion. In the acidic environment, it's easier to form gallium ions. Due to the auxo-action of Ga ions and increasing in positive charge, so that the adsorption for dye is shortened. In a neutral solution, the oxide layer is easier to be formed, while without too much Ga ions. That's why the adsorption time is longer than in acidic solution. Notably, in an alkaline environment, the reaction (4) will be enhanced and reaction (5) will be suppressed, so that more GaOOH will be formed and then react with PS to get new product, which maybe metal complex dye (Scheme 1) as described in literature [33,34]. Based on this phenomenon, it could be got different products through adjust pH value, which is valuable for the exploration of interfacial property and for the synthesis of a new metal complex dye. As depicted in Fig. 4d, the adsorption time is also shortened with temperature increasing. With the increase of temperature, except for promoting molecular motion, it also enhances oxygen permeability enabling further oxidation. It was proved and called thermal-oxidative compositional inversion (TOCI) process by Martin Thuo's group [48]. The adsorption process also supports this discovery. As presumed above, the ionic strength could accelerate the adsorption process. As expected, shown in Fig. 4e, when added the ionic concentration $\leq$0.5 M, the adsorption rate is accelerated obviously. When >0.5 M, there will be little impact, which maybe means that the excess ion will not stimulate the adsorption due to the limitation of PS. Apparently, the adsorption is promoted by the factors mentioned above, which further confirms our analysis of adsorption mechanism. Furthermore, these phenomena could be used for different products and promote the exploration of surface functionalization.

To detect the recycling capability of this system, it can be seen that in 10 cycle number there is little influence on cyclic adsorption (Fig. 4f). Precisely, based on the adsorption mechanism, it can adsorb as long as oxide layer exist. In other words, with the oxide layer regenerated spontaneously, liquid metal can be used for adsorption until it's degraded completely, which is according with the concept of sustainability.

Furthermore, to explore the adsorption dynamics, the solutions were picked out at different minutes during the process to detect the UV-Vis spectrum shown in Fig. 4g. Fig. 4h is the enlarged view from 420–580 nm. It could be seen that the adsorption peak of PS (506 nm) in the preliminary stage decreased little, which suggests the PS is adsorbed very slowly. In the later stage of adsorption, after around 90 min, the adsorption becomes quicker, which the concentration tends to hardly be detected. The reason maybe that at first the oxide layer is rarely existing due to the effect of acetic acid in PS solution. After the dissolution of oxygen and intermolecular contact, the oxide layer with defect structure forms and the PS is adsorbed quickly. Moreover, the removal efficiency was calculated based on Eq. (1). It could be seen clearly in Fig. 4i that the removal efficiency of PS was slowly in less than 90 min, and after that the adsorption was changed quickly. This phenomenon is consistent with the analyzation of adsorption mechanism. It is worth noting that the adsorption capacity as a function of time

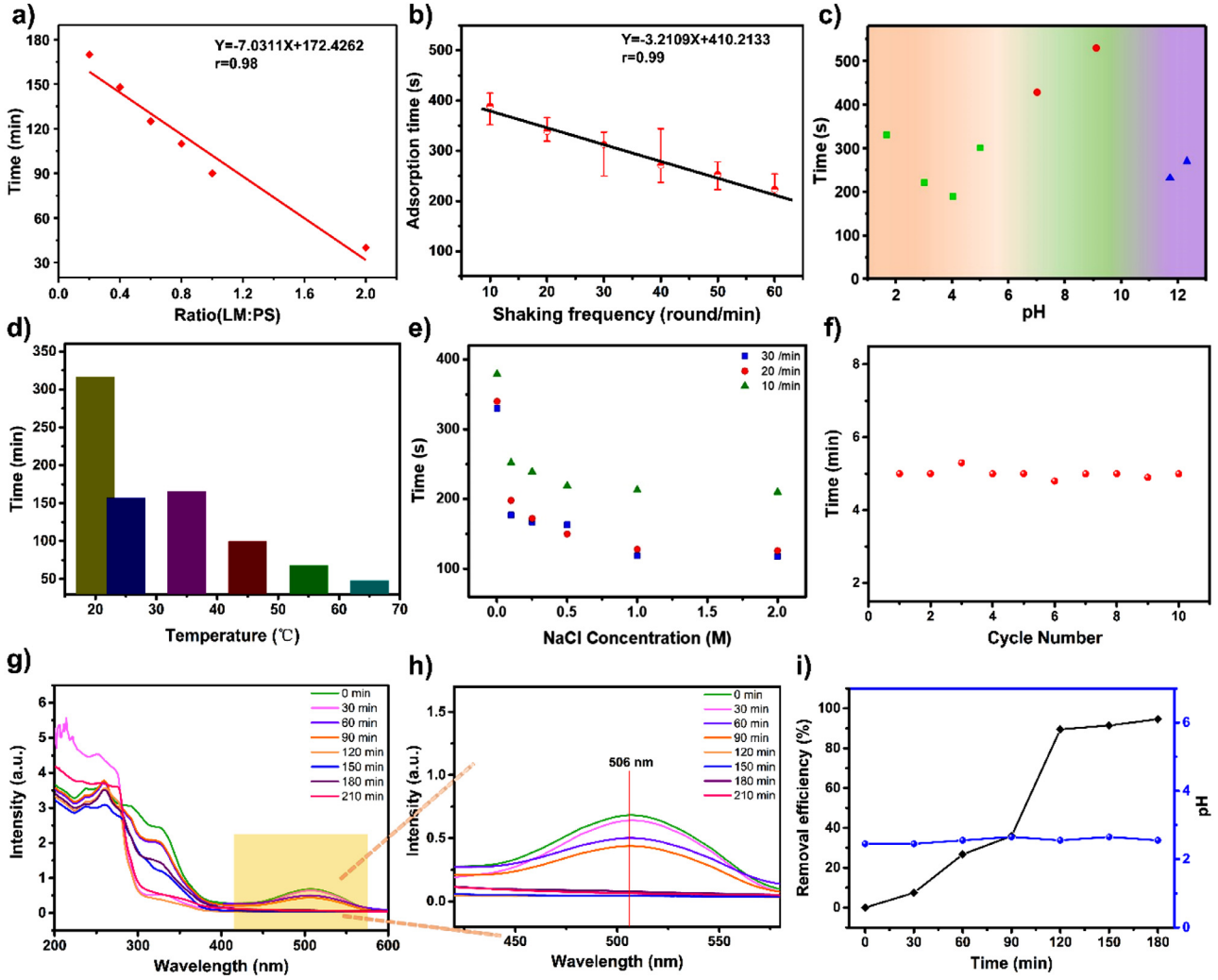

Fig. 4. Relationship between adsorption equilibrium time and LM:PS ratio (a), shaking frequency (b), pH (c), the last two values are the time for the solution turning to yellow), temperature (d), ion concentration (e), cycle number (f). UV-Vis spectroscopy (g, h), removal efficiency and pH (i) of the solution at different time (For interpretation of the references to color in this figure legend, the reader is referred to the web version of this article.).

(q_t) could be calculated according to the equation: $q_t = (C_0 - C_t)$ V/m, where C_0 is the concentration of the dye (mg/L) at 0 min. C_t is the concentration of the dye (mg/L) at t min. V is the volume of the solution (L) and m is the mass of the adsorbent (g) [19]. As shown in Table 1, we compare the adsorption capacity of liquid metal with different adsorbents toward PS dye. It is calculated roughly that at least 50 mL PS is adsorbed by 100 μL LM (about 83.3 mg/g). Due to the large density of gallium-based liquid metal (around 6.0 g•cm^{-3}), it was considered inappropriate to use this equation to compare with other adsorbents. Further researches on light-liquid metal composites will be progressed in the future. Even so, gallium-based liquid metals show many advantages, such as excellent reconfigurable ability, simple preparation process, easy to recycle, which may exert important function in certain circumstances. For example, when the dye solution is stored at tortuous and narrow place, reconfigurable liquid metal could be used simply to execute the adsorption process. After adsorption, it could be easily removed just by injection syringe or other methods as a whole. Especially, in some extreme circumstances liquid metal could realize the solid-liquid phase change with adsorption ability similarly. Moreover, conductivity and adsorption can be synergistically used for real-time monitoring as descripted in Fig. 5. Thus, we believe this reconfigurable gallium-based absorbent could have great prospect in some practical applications, such as soft robotics, wearable devices and so on.

As known that the surface oxide layer on liquid metal will affect the interfacial impedance [51], as a proof of concept, the impedance during the adsorption process is detected in this work. The schematic diagram of EIS measurement in our experiment is shown in Fig. 5a,c, where two droplets of the liquid metal with surface oxide are at both sides of a tube and the PS solution is in the middle. Here the two LM parts work as electrodes. The surface oxide works as the absorbing membrane and PS is the measured analyte. EIS measurement experiments at different time are shown in Fig. 5b, the color change could be seen in silicone tube with the adsorption. The equivalent circuit of the whole system is shown in Fig. 5d, in which R_{LM} is the resistance of LM, which is negligible. R_{SO1} and R_{SO2} represent the polarization resistance of surface oxide. C_{SO1} and C_{SO2} represent the capacitance of the double layer of charge induced by the accumulation of ions in the solution in proximity to the electrode. The R_{PS} represents resistance of the PS solution. Based on our analysis, the adsorption of PS by surface oxide is due to the electrostatic attraction, which is a physical combination. Thus, the R_{SO1} and R_{SO2} should alter during the adsorption process. The R_{PS} should also change as PS decrease in solution. According to this theoretical analysis, the whole

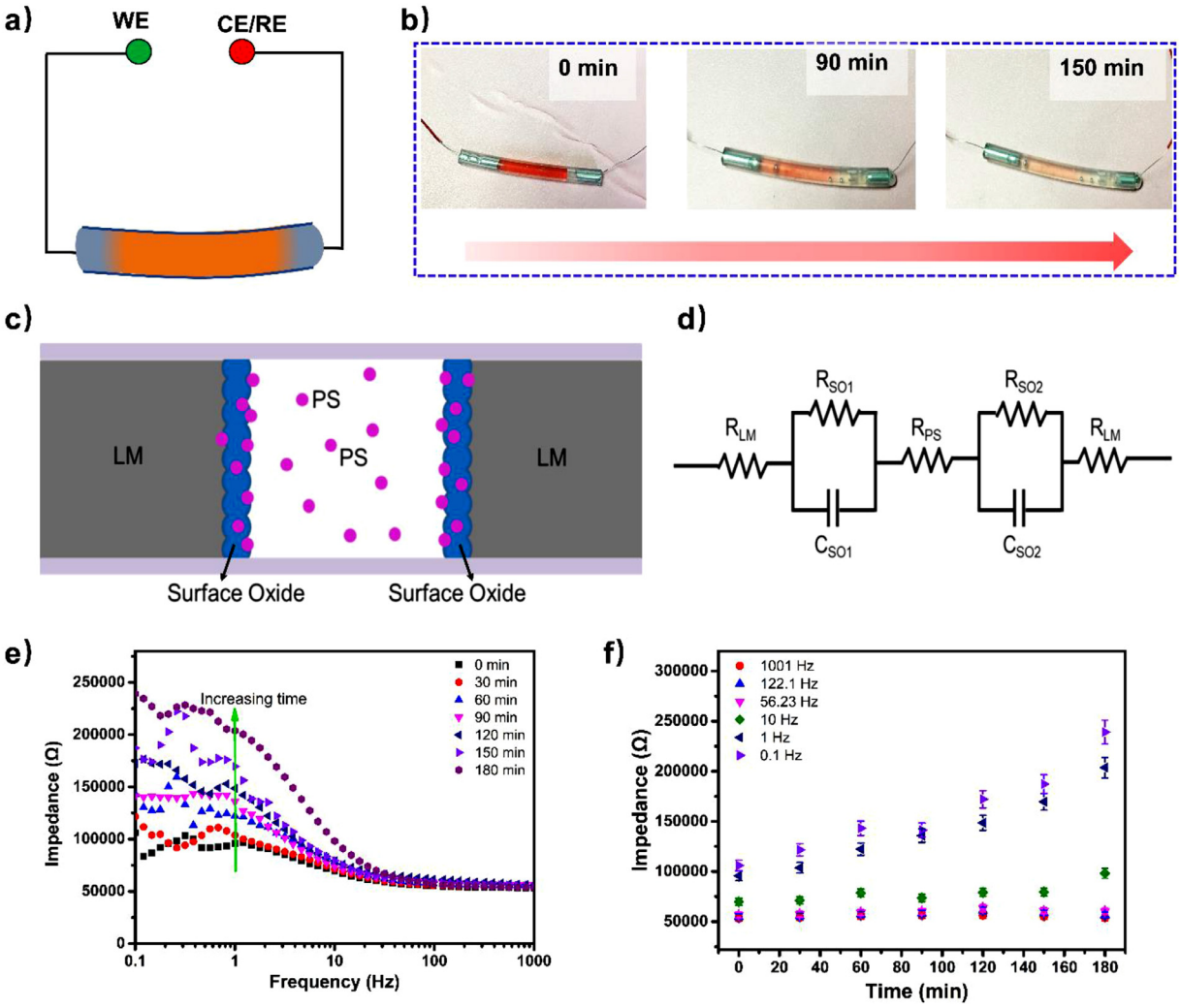

Fig. 5. Schematic diagram of EIS measurement (a). Photograph of interfacial impedance test at different time (b). Illustration of LM and PS in a tube (c). Equivalent circuit of the whole system (d). Relationship between impedance and frequency at different time (e), adsorption time (f).

readout of the impedance should change during the PS adsorption process.

To realize the monitoring of adsorption of PS, we measured the system impedance correlated with varied frequencies in every 30 min during the whole adsorption process (about 180 min). In general, the impedance decreased with the increasing frequency as depicted in Fig. 5e, which suggests the resistive impedance decreased at high frequencies. At low frequencies, however, the measured impedance has obviously increase during adsorption process. In other words, it appears that the impedance increases with the decrease of PS concentration during the adsorption process, which suggests the PS adsorption can be monitored and quantified in real-time. To illustrate the change more clearly, the impedance at various frequencies during the adsorption process was recorded in Fig. 5f. At high frequencies, the interface impedance has very slight increase during the adsorption. However, it shows pronounced increase (from 100000 to 200000 Ω, rate of change 50%) in impedance at low frequency (1 and 0.1 Hz). This result suggests the adsorption of PS could obviously influence the resistive impedance in this system including R_{SO1}, R_{SO2} and R_{PS}. This result is also consistent with our assumption that the adsorption of PS by the oxide and the removal of PS in the solution are generally physical process, which should largely influence the resistance of the system. To further clarify the relation between the system impedance increase and the PS adsorption process, the platinum (Pt) electrodes are used as control and the EIS measurement in PS solution is carried out. The Pt electrodes should have little capacity in PS adsorption. The EIS results also confirmed that the impedance remained almost unchanged for 180 min in HAc and PS solution, respectively (Fig. S8), which suggest no obvious physical or chemical process in relation to PS occurred. We also compared the impedance spectrum of Pt electrode in pure solvent (0.5% HAc) and in PS solution (Fig. S7). The results suggest the electrolyte component variation (mainly RPS) indeed has certain influence on the whole impedance (from 4000 to 4800 Ω, rate of change 20%). These control experimental results prove from another side that both the adsorption of PS by gallium oxide (R_{SO1}, R_{SO2}) and the removal of PS (R_{PS}) contribute to the impedance increase at low frequencies. Besides, the impedance readout has a generally linear relation with the increasing time at low frequency when PS is continuously being absorbed. As a whole, this simple device is proved to be efficient in monitoring the PS adsorption process using EIS technique. Thus, this impedance sensing assay not only provides an electrical quantification of this PS adsorption but also further reveals and proves the adsorption mechanism in an electrochemical way. Creatively, taking advantages of the electrical conductivity of liquid metal as electrodes, the adsorption process can be detected by the EIS technique, which indeed provides a simple and

real-time quantification method for PS adsorption without additional electrodes and adsorbents. This study also puts forward to a new consideration on multifunctional electrode.

As described above, it is proved that the reconfigurable gallium-based liquid metal and its oxide system can effectively adsorb PS with remarkable advantages such as simple regeneration and recycling, energy and time saving and eco-friendly. Interestingly, through controlling the pH, a new metal complex dye maybe synthesized, which will be valuable in chemical engineering and greatly expand the application of gallium oxide layer. This adsorption process of this kind of reconfigurable materials can inspire further applications such as: (i) preparation of adsorbed cloth, which can be used in western blotting through the way of interlining using their high adsorbent property to reduce the damage of PS to human health and environment. (ii) design of electrical and chemical sensors to monitor or detect some components even in blood, sweat, urine. (iii) preparation of large-scale materials, in view of the solidified liquid metal, which can be directly used for free-standing and easily recycled adsorption/sensor materials in wide ambient environment.

4. Conclusion

In summary, we report a reconfigurable and sustainable gallium-based liquid metal oxide for effective adsorption of the biological dye PS in an economical and convenient way. The surface characterization results confirmed the existence of the gallium oxide in combination of PS. The quantitative experiments on various adsorption conditions further prove the oxide layer acts as the adsorbent. Meanwhile, Ga ion is also revealed to promote the adsorption in some degree. During the adsorption process, the gallium oxide skin over the flowing liquid metal is easily reconfigurable and continuously producible. Thus, this brand-new adsorbent maintains effectivity until it is degraded completely, which is in accord with the concept of sustainability. The adsorption process is time and energy saving, which may extend its application from laboratory to industry. Combined with excellent electrical conductivity of liquid metal, the PS adsorption process could be electrically measured by impedance sensing technology, which presents a novel and simple chemical sensing system for more possible applications. Above all, this study not only provides an effective and novel adsorbent material for dye removal, but also burst more inspirations on adsorbent material design, chemical engineering and molecular sensing and monitoring.

Declaration of Competing Interest

The authors declare that they have no known competing financial interests or personal relationships that could have appeared to influence the work reported in this paper.

CRediT authorship contribution statement

Xinpeng Wang: Conceptualization, Visualization, Formal analysis, Writing – original draft. **Hongzhang Wang:** Visualization. **Kang Sun:** Visualization. **Wanjun Li:** Formal analysis. **Xuanqi Chen:** Visualization. **Liang Hu:** Supervision, Writing – review & editing. **Yubo Fan:** Supervision, Writing – review & editing.

Acknowledgments

This work is supported by the National Natural Science Foundation of China (Grant Nos. 81801794, U20A20390, 11827803) and the Beijing Natural Science Foundation (Grant No. 7202104).

Supplementary materials

Supplementary material associated with this article can be found, in the online version, at doi:10.1016/j.apmt.2021.101265.

References

[1] S.Y. Jeon, S.H. Kang, Electrochemical morphing, Nature 573 (2019) 205–213, doi:10.1038/s41586-019-1538-z.
[2] Y. Lu, Q. Hu, Y. Lin, D.B. Pacardo, C. Wang, W. Sun, F.S. Ligler, M.D. Dickey, Z. Gu, Transformable liquid-metal nanomedicine, Nat. Commun. 6 (2015) 10066, doi:10.1038/ncomms10066.
[3] Y. Zhang, N. Zheng, Y. Cao, F. Wang, P. Wang, Y. Ma, B. Lu, G. Hou, Z. Fang, Z. Liang, M. Yue, Y. Li, Y. Chen, J. Fu, J. Wu, T. Xie, X. Feng, Climbing-inspired twining electrodes using shape memory for peripheral nerve stimulation and recording, Sci. Adv. 5 (2019) eaaw1066, doi:10.1126/sciadv.aaw1066.
[4] M. Zhang, R. Guo, K. Chen, Y. Wang, J. Niu, Y. Guo, Y. Zhang, Z. Yin, K. Xia, B. Zhou, H. Wang, W. He, J. Liu, M. Sitti, Y. Zhang, Microribbons composed of directionally self-assembled nanoflakes as highly stretchable ionic neural electrodes, Proc. Natl. Acad. Sci. U. S. A. 117 (2020) 14667–14675, doi:10.1073/pnas.2003079117.
[5] S.M. Ali, C. Sovuthy, M.A. Imran, S. Socheatra, Q.H. Abbasi, Z.Z. Abidin, Recent advances of wearable antennas in materials, fabrication methods, designs, and their applications: state-of-the-art, Micromachines 11 (2020) 888 (Basel), doi:10.3390/mi11100888.
[6] E.J. Markvicka, M.D. Bartlett, X. Huang, C. Majidi, An autonomously electrically self-healing liquid metal-elastomer composite for robust soft-matter robotics and electronics, Nat. Mater. 17 (2018) 618–624, doi:10.1038/s41563-018-0084-7.
[7] M.D. Dickey, A river (of liquid metal) runs through it, Natl. Sci. Rev. 7 (2020) 721–722, doi:10.1093/nsr/nwaa018.
[8] K. Han, G. Kokot, S. Das, R.G. Winkler, G. Gompper, A. Snezhko, Reconfigurable structure and tunable transport in synchronized active spinner materials, Sci. Adv. 6 (2020) eaaz8535, doi:10.1126/sciadv.aaz8535.
[9] S. Cotillas, J. Llanos, P. Cañizares, D. Clematis, G. Cerisola, M.A. Rodrigo, M. Panizza, Removal of procion red MX-5B dye from wastewater by conductive-diamond electrochemical oxidation, Electrochim. Acta 263 (2018) 1–7, doi:10.1016/j.electacta.2018.01.052.
[10] H. Sander, S. Wallace, R. Plouse, S. Tiwari, A.V. Gomes, Ponceau S waste: Ponceau S staining for total protein normalization, Anal. Biochem. 575 (2019) 44–53, doi:10.1016/j.ab.2019.03.010.
[11] M. Clark, Handbook of Textile and Industrial Dyeing, Woodhead Publishing, 2011.
[12] J.M. Samet, W.A. Chiu, V. Cogliano, J. Jinot, D. Kriebel, R.M. Lunn, F.A. Beland, L. Bero, P. Browne, L. Fritschi, J. Kanno, D.W. Lachenmeier, Q. Lan, G. Lasfargues, F.Le Curieux, S. Peters, P. Shubat, H. Sone, M.C. White, J. Williamson, M. Yakubovskaya, J. Siemiatycki, P.A. White, K.Z. Guyton, M.K. Schubauer-Berigan, A.L. Hall, Y. Grosse, V. Bouvard, L. Benbrahim-Tallaa, F. El Ghissassi, B. Lauby-Secretan, B. Armstrong, R. Saracci, J. Zavadil, K. Straif, C.P. Wild, The IARC monographs: updated procedures for modern and transparent evidence synthesis in cancer hazard identification, J. Natl. Cancer Inst. 112 (2020) 30–37, doi:10.1093/jnci/djz169.
[13] W.H. Organization(WHO), in: IARC Monographs on the Identification of Carcinnogenic Hazards to Humans, Agents Classified by the IARC Monographs, 2020, pp. 1–128.
[14] N.B. Singh, G. Nagpal, S. Agrawal, Rachna, Water purification by using adsorbents: a review, Environ. Technol. Innov. 11 (2018) 187–240, doi:10.1016/j.eti.2018.05.006.
[15] M. Mokhtar, Application of synthetic layered sodium silicate magadiite nanosheets for environmental remediation of methylene blue dye in water, Materials 10 (2017) (Basel), doi:10.3390/ma10070760.
[16] M.A. Salam, M. Mokhtar, S.M. Albukhari, D.F. Baamer, L. Palmisano, M.R. Abukhadra, Insight into the role of the zeolitization process in enhancing the adsorption performance of kaolinite/diatomite geopolymer for effective retention of Sr (II) ions; batch and column studies, J. Environ. Manag. 294 (2021) 112984, doi:10.1016/j.jenvman.2021.112984.
[17] M.A. Salam, A.A. Alshehri, W. Schwieger, M. Mokhtar, Removal of bismuth ions utilizing pillared ilerite nanoclay: kinetic thermodynamic studies and environmental application, Microporous Mesoporous Mater. 313 (2021) 110826, doi:10.1016/j.micromeso.2020.110826.
[18] T.G. Venkatesha, Y.A. Nayaka, B.K. Chethana, Adsorption of Ponceau S from aqueous solution by MgO nanoparticles, Appl. Surf. Sci. 276 (2013) 620–627, doi:10.1016/j.apsusc.2013.03.143.
[19] X. Wang, Z. Liu, X. Ye, K. Hu, H. Zhong, J. Yu, M. Jin, Z. Guo, A facile one-step approach to functionalized graphene oxide-based hydrogels used as effective adsorbents toward anionic dyes, Appl. Surf. Sci. 308 (2014) 82–90, doi:10.1016/j.apsusc.2014.04.103.
[20] A. Flilissa, S. Venkataraman, K. Laouameur, A. Beroual, O. Flilissa, K. Omine, T. Chaabane, A. Darchen, Surface modification of aluminum phosphate by sodium dodecylbenzenesulfonate (SDBS): a new nano-structured adsorbent for an improved removal of Ponceau S, J. Environ 8 (2020) 103625, doi:10.1016/j.jece.2019.103625.
[21] Hyang-HoonChae Hyun-JaeShin, Removal of Ponceau S from aqueous solutions by organic clay, J. Biosci. Bioeng. 108 (2009) S85–S86, doi:10.1016/j.jbiosc.2009.08.251.

[22] J. de Jesus da Silveira Neta, G. Costa Moreira, C.J. da Silva, C. Reis, E.L. Reis, Use of polyurethane foams for the removal of the direct red 80 and reactive blue 21 dyes in aqueous medium, Desalination 281 (2011) 55–60, doi:10.1016/j.desal.2011.07.041.
[23] A. Kamari, W.S.W. Ngah, L.K. Liew, Chitosan and chemically modified chitosan beads for acid dye sorption, J. Environ. Sci. 21 (2009) 296–302 (China), doi:10.1016/S1001-0742(08)62267-6.
[24] Z. Zhu, P. Wu, G. Liu, X. He, B. Qi, G. Zeng, W. Wang, Y. Sun, F. Cui, Ultrahigh adsorption capacity of anionic dyes with sharp selectivity through the cationic charged hybrid nanofibrous membranes, Chem. Eng. J. 313 (2017) 957–966, doi:10.1016/j.cej.2016.10.145.
[25] C. Amy, D. Budenstein, M. Bagepalli, D. England, F. DeAngelis, G. Wilk, C. Jarrett, C. Kelsall, J. Hirschey, H. Wen, A. Chavan, B. Gilleland, C. Yuan, W.C. Chueh, K.H. Sandhage, Y. Kawajiri, A. Henry, Pumping liquid metal at high temperatures up to 1673 kelvin, Nature 550 (2017) 199–203, doi:10.1038/nature24054.
[26] L. Hu, L. Wang, Y. Ding, S. Zhan, J. Liu, Manipulation of liquid metals on a graphite surface, Adv. Mater. 28 (2016) 9210–9217, doi:10.1002/adma.201601639.
[27] M.D. Dickey, Stretchable and soft electronics using liquid metals, Adv. Mater. 29 (2017) 1606425, doi:10.1002/adma.201606425.
[28] M.A. Creighton, M.C. Yuen, M.A. Susner, Z. Farrell, B. Maruyama, C.E. Tabor, Oxidation of gallium-based liquid metal alloys by water, Langmuir 36 (2020) 12933–12941, doi:10.1021/acs.langmuir.0c02086.
[29] J.H. Fu, T.Y. Liu, Y. Cui, J. Liu, Interfacial engineering of room temperature liquid metals, Adv. Mater. Interfaces 8 (2021) 2001936, doi:10.1002/admi.202001936.
[30] H. Li, R. Qiao, T.P. Davis, S.Y. Tang, Biomedical applications of liquid metal nanoparticles: a critical review, Biosensors 10 (2020) (Basel), doi:10.3390/bios10120196.
[31] J. Yan, Y. Lu, G. Chen, M. Yang, Z. Gu, Advances in liquid metals for biomedical applications, Chem. Soc. Rev. 47 (2018) 2518–2533, doi:10.1039/C7CS00309A.
[32] Z. Wang, X. Chen, F.F. Ren, S. Gu, J. Ye, Deep-level defects in gallium oxide, J. Phys. D Appl. Phys. 54 (2021) 043002, doi:10.1088/1361-6463/abbeb1.
[33] B.R. Kirthan, M.C. Prabhakara, H.S.B. Naik, P.H.A. Nayak, E.I. Naik, Synthesis, characterization, DNA interaction and anti-bacterial studies of Cu(ii), Co(ii) and Ni(ii) metal complexes containing azo-dye ligand, Chem. Data Collect. 29 (2020) 100506, doi:10.1016/j.cdc.2020.100506.
[34] R. Kılınçarslan, E. Erdem, H. Kocaokutgen, Synthesis and spectral characterization of some new azo dyes and their metal complexes, Transition Met. Chem. 32 (2006) 102–106, doi:10.1007/s11243-006-0134-x.
[35] T. Daeneke, K. Khoshmanesh, N. Mahmood, I.A. de Castro, D. Esrafilzadeh, S.J. Barrow, M.D. Dickeyb, K. Kalantar-zadeh, Liquid metals fundamentals and applications in chemistry, Chem. Soc. Rev. 47 (2018) 4073–4111, doi:10.1039/C7CS00043J.
[36] X. Wang, L. Li, X. Yang, H. Wang, J. Guo, Y. Wang, X. Chen, L. Hu, Electrically induced wire-forming 3D printing technology of gallium-based low melting point metals, Adv. Mater. Technol. (2021) 2100228 n/a, doi:10.1002/admt.202100228.
[37] J. Tang, S. Lambie, N. Meftahi, A.J. Christofferson, J. Yang, M.B. Ghasemian, J. Han, F.M. Allioux, M.A. Rahim, M. Mayyas, T. Daeneke, C.F. McConville, K.G. Steenbergen, R.B. Kaner, S.P. Russo, N. Gaston, K. Kalantar-Zadeh, Unique surface patterns emerging during solidification of liquid metal alloys, Nat. Nanotechnol. 16 (2021) 431–439, doi:10.1038/s41565-020-00835-7.
[38] E. Huang, J. Li, G. Wu, W. Dai, N. Guan, L. Li, A simple synthesis of Ga_2O_3 and GaN nanocrystals, RSC Adv. 7 (2017) 47898–47903, doi:10.1039/c7ra10639d.
[39] J. Xiong, J. Yan, C. Li, X. Wang, L. Wang, D. Pan, Y. Xu, F. Wang, X. Li, Q. Wu, J. Liu, Y. Liu, Q. Liu, Y. Zhou, M. Yang, Injectable liquid metal nanoflake hydrogel as a local therapeutic for enhanced postsurgical suppression of tumor recurrence, Chem. Eng. J. 416 (2021) 129092, doi:10.1016/j.cej.2021.129092.
[40] H.S. Casalongue, S. Kaya, V. Viswanathan, D.J. Miller, D. Friebel, H.A. Hansen, J.K. Nørskov, A. Nilsson, H. Ogasawara, Direct observation of the oxygenated species during oxygen reduction on a platinum fuel cell cathode, Nat. Commun. 4 (2013), doi:10.1038/ncomms3817.
[41] Y. Liu, J. Li, W. Zhang, Liquid metal exfoliation of two dimensional polydopamine nanosheets for templated assembly of noble metal nanoparticles, Chem. Commun. 56 (2020) 6229–6232 (Camb.), doi:10.1039/d0cc02108c.
[42] H.J. Bae, T.H. Yoo, Y. Yoon, I.G. Lee, J.P. Kim, B.J. Cho, W.S. Hwang, High-aspect ratio β-Ga_2O_3 nanorods via hydrothermal synthesis, Nanomaterials 8 (2018) (Basel), doi:10.3390/nano8080594.
[43] M. Gopalakrishnan, V. Purushothaman, V. Ramakrishnan, G.M. Bhalerao, K. Jeganathan, The effect of nitridation temperature on the structural, optical and electrical properties of GaN nanoparticles, CrystEngComm 16 (2014) 3584–3591, doi:10.1039/c3ce42417k.
[44] Y. Ding, M. Zeng, L. Fu, Surface chemistry of gallium-based liquid metals, Matter 3 (2020) 1477–1506, doi:10.1016/j.matt.2020.08.012.
[45] M.D. Dickey, Emerging applications of liquid metals featuring surface oxides, ACS Appl. Mater. Interfaces 6 (2014) 18369–18379, doi:10.1021/am5043017.
[46] H. Song, T. Kim, S. Kang, H. Jin, K. Lee, H.J. Yoon, Ga-based liquid metal micro/nanoparticles: recent advances and applications, Small 16 (2019) e1903391, doi:10.1002/smll.201903391.
[47] L. Li, H. Chang, N. Yong, M. Li, Y. Hou, W. Rao, Superior antibacterial activity of gallium based liquid metals due to Ga(3+) induced intracellular ROS generation, J. Mater. Chem. B 9 (2021) 85–93, doi:10.1039/d0tb00174k.
[48] A. Martin, W. Kiarie, B. Chang, M. Thuo, Chameleon metals: autonomous nanotexturing and compositioninversion on liquid metals surfaces, Angew. Chem. 59 (2019) 352–357, doi:10.1002/anie.201912639.
[49] B.N. Patil, D.B. Naik, V.S. Shrivastava, Photocatalytic degradation of hazardous Ponceau-S dye from industrial wastewater using nanosized niobium pentoxide with carbon, Desalination 269 (2011) 276–283, doi:10.1016/j.desal.2010.11.014.
[50] J. Chen, Q. Cao, X. Han, Smart water-based ferrofluid with stable state transition property: Preparation and its application in anionic dye removal, J. Clean. Prod. 287 (2021) 125003, doi:10.1016/j.jclepro.2020.125003.
[51] T. Shay, O.D. Velev, M.D. Dickey, Soft electrodes combining hydrogel and liquid metal, Soft Matter 14 (2018) 3296–3303, doi:10.1039/c8sm00337h.